

# Studies of the Precision of Proton Beam Profile Monitor SEM's

5 January 2005

Sacha E. Kopp, Zarko Pavlovic  
University of Texas at Austin

## 1 Introduction

Segmented secondary emission monitors (SEMs) will be used in 10 stations along the NuMI beamline to monitor the primary proton beam size along the transport from the Main Injector to the NuMI target. The target is 2 cm high and 6.4 mm wide. The width of the beam that will be used in NuMI will be 1 mm along most of the transport line. A narrower beam could damage the target, while a wider beam could result in some protons missing the target. Eight of the SEM's will have 1 mm pitch, hopefully sufficient to measure position with a precision of 100  $\mu\text{m}$ , and two of the SEM's, those located just upstream of the target, have to 0.5 mm pitch, in order to measure the beam position with the precision of 50  $\mu\text{m}$ .

A prototype SEM was tested in the MiniBooNE beam transport line in May 2003. While the MiniBooNE beam parameters differ from those anticipated for NuMI (see Table 1), this beam line permitted early verification of the foil SEM design. Some differences, listed in Table 2, exist between the foils designed for the prototype SEM and the final SEM chambers installed in the NuMI line. Further details of the prototype design are given in Ref. [1], while the final SEM design description can be found in Ref [2].

During the beam tests, the SEM was successfully used to measure beam size at one location in the MiniBooNE line. It was also capable of measuring beam centroid position. Because it was the only profile monitor in that portion of the transport line, no independent measurement existed to corroborate the prototype's beam size measurements. A pair of nearby "Beam Position Monitors (BPM's)" was able to corroborate the SEM's beam centroid measurement. Like beam profile, the beam centroid resolution can be related to several key aspects of the SEM design, such as readout noise and the accuracy of the segmented SEM grid assembly. In this note, we analyze the SEM's centroid position precision during the MiniBooNE run. These measurements are compared to calculations of expected centroid resolution performance in Section 4. Following the validation of the calculations using the test beam data, the same code is used to calculate the expected beam size resolution achievable from the SEM's.

	MiniBooNE	NuMI
Proton energy ( $GeV$ )	8	120
Intensity ( $\times 10^{12}$ ppp)	5	40
Spill Rate ( $Hz$ )	5	0.5
Spill Duration ( $\mu s$ )	1.56	8.67
Horizontal beam size ( $mm$ )	$\sim 6$	$\sim 1$
Vertical beam size ( $mm$ )	$\sim 3$	$\sim 1$

Table 1: Comparison of MiniBooNE and NuMI beamlines.

## 2 Data analysis

We looked at the data from seven runs taken in the fall of 2003. Most of the runs contained over 15000 proton spills. Only the data when the beam intensity was sufficiently high ( $\sim 10^{12}$  ppp) was used in the analysis. Data from several beam line instruments was read out through ACNET and written to two separate files. One contained data from various devices and the other contained the SEM data. At the readout of each beam device, the ACNET front end placed a timestamp of the readout time and this timestamp was included in the data files. It was noticed that the timestamps haven't always matched and after some time the two data files become out of synchronization. Because of that the data had to be sorted first and only the lines when in both files closely matching timestamps could be found were taken. After these cuts there were 79658 spills with useful data.

Figure 1 shows the beam line near the SEM and Table 3 gives the explanation of the symbols. Immediately after our prototype there was a vertical BPM, while between the SEM and the nearest horizontal BPM there were a couple of quadrupole magnets. To analyse the SEM data we wanted to correlate it with BPM data. However, there is no simple linear relation between all the BPM and SEM data. Changing magnet currents, beam position and intensity causes both the slope and the offset in the relation between SEM and BPM to change. The situation is worse for horizontal than for vertical plane since as mentioned there are magnets in between the SEM prototype and horizontal BPM.

The data analysed was split in parts during which the current in nearby magnets was almost constant. One other condition was that the beam intensity was more or less constant in a given time interval under study. The instrument Tor860 was used for intensity monitoring.

	Prototype	SEM	Fine resolution SEM
Strip width (mm) - over the aperture	0.75	0.15	0.25
Strip pitch (mm)	1	1	0.5
Foil thickness ( $\mu m$ )	5	5	5

Table 2: Comparison of the prototype and the SEMs that are going to be used in NuMI beamline.

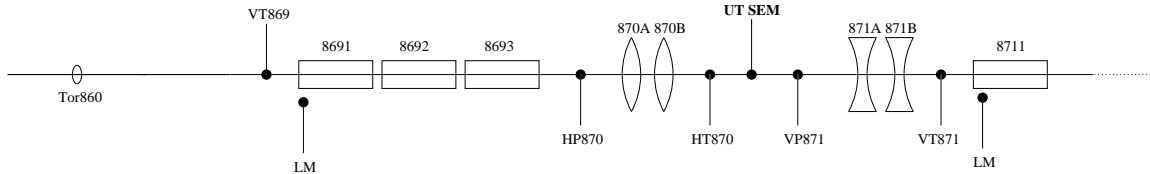


Figure 1: Beamline segment around SEM prototype.

Figure 2 shows one example of the horizontal and vertical beam profiles as seen by the SEM after one spill. The vertical axis on these plots is the pulse height from a given strip[3]. The beam was broader in horizontal plane and narrower in the vertical plane. The data were fitted with Gaussians and parameters for this particular spill are given in the plots. Both horizontal and vertical beam width roughly agree with the MiniBoone beam parameters given in Table 1. The beam intensity during that spill was  $4.5 \times 10^{12}$  ppp (protons per pulse).

### 3 Measured SEM Centroid Resolution

As mentioned, while the SEM resolution on beam width is of interest, only the centroid position resolution could be studied during this test owing to the availability of other instrumentation in the MiniBoone line. This section describes the method of measuring the centroid position resolution.

The centroid resolution of the SEM depends upon the width of the beam, the intensity of the beam, and upon the electronics readout noise on the SEM channels. The beam width in vertical plane was nearly constant at  $\sigma_x = 3.44 \pm 0.09$  during the 80000 spills that were considered, while the horizontal beam size varied between two values,  $\sigma_y = 7.4$  mm and  $\sigma_y = 8.2$  mm, during the test period, varying as a function of the beam intensity. This gives us 3 different beam widths for which we try to find the SEM centroid precision.

To find the SEM resolution in the MiniBoone data we performed three estimates. First, we compare the beam position as measured by the SEM and a nearby BPM; the residuals

Device name	Description
Tor	Toroid
LM	Loss monitor
HP	Horizontal position monitor
VP	Vertical position monitor
HT	Horizontal trim magnet
VT	Vertical trim magnet
UT SEM	UT Multiwire SEM

Table 3: Description of devices.

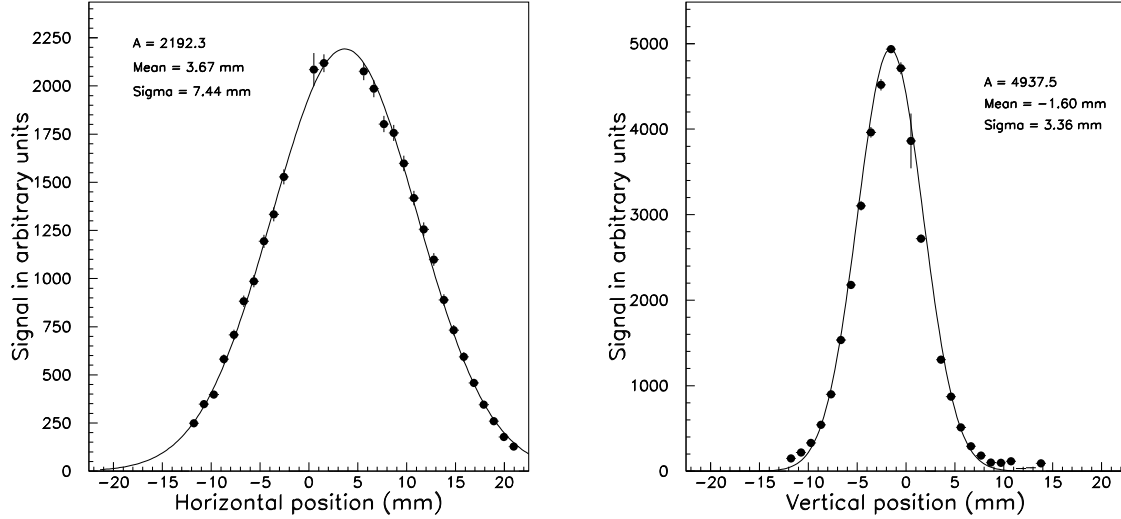


Figure 2: Horizontal and vertical beam profiles during one spill.

in a scatter plot of the two positions provides an upper bound on the SEM resolution. The second estimate is derived from periods of time during the run in which the beam position was relatively constant; the RMS spread of beam spill centroid positions again provides an upperbound on the SEM (and BPM) resolution. The third estimate attempts to combine the above two studies to estimate a best estimate of the SEM resolution.

### 3.1 Study #1

The vertical beam measurement is easiest to proceed with, given that no focusing devices are present between the BPM and SEM. Thus, the two devices may be correlated rather easily. We start by assuming that the BPM and the SEM have same resolution. If we look at the SEM data plotted versus the BPM data we see that the data points are scattered around a line (Figure 3). In the case when the two devices would have infinite precision we would expect for the data points to lie exactly on the line. Because the resolutions of the BPM and the SEM are finite we see the data points scattered around the line. The residuals of the data from the best fit line are shown in Figure 3, and have an RMS of  $127 \mu m$ . The residuals should be a measure of the two devices' resolutions, added in quadrature:

$$\sqrt{\sigma_{SEM}^2 + \sigma_{BPM}^2} = 127 \mu m. \quad (1)$$

If both devices contribute equally to the residuals, *ie.* both SEM and BPM have the same resolution, then we would have

$$\sigma_{BPM} = \sigma_{SEM} = \frac{127 \mu m}{\sqrt{2}} = 90 \mu m \quad (2)$$

However, two facts indicate that the above estimate is only an upper bound, and in fact the SEM resolution is smaller than  $90 \mu\text{m}$ . The first fact is that the slope of the fitted line in Figure 3 is greater than 1.0, indicating that some scale factor exists between a displacements measured in the BPM and those measured in the SEM. The origin of this scale factor is unknown, but may be as simple as an electronics miscalibration.

The second fact in support of a smaller SEM resolution comes from the second resolution estimate performed. In the second estimate, we looked at the data in time intervals during which the beam is continuously hitting almost at the same position on the foils. Normally, the beam does wander in both the vertical and horizontal directions as a function of time, as shown in Figure 4. However, with a suitable choice of spill numbers, we can select a period in which the beam position is *nearly* constant. Figure 5 shows one such interval of data (spill range shown is 35910-37240). The RMS of the beam centroid positions spill-to-spill is a measure of both the beam wandering and the device resolution, *ie.*

$$RMS_{SEM} = \sqrt{\sigma_{SEM}^2 + \sigma_{wander}^2} \quad (3)$$

$$RMS_{BPM} = \sqrt{\sigma_{BPM}^2 + \sigma_{wander}^2}$$

where  $\sigma_{wander}$  is a measure of the RMS variation of the beam position on a detector over a period of time due to variations in the beamline performance, and  $\sigma_{BPM,SEM}$  are the intrinsic device resolutions. The quantity  $\sigma_{wander}$  is not *a priori* known and varies from time interval to time interval but it should be the same for both devices. However, as may be seen in Figure 5, the BPM spread is systematically larger than the SEM spread. Given the same beam wandering on both devices, it appears evident that  $\sigma_{SEM} < \sigma_{BPM}$ .

## 3.2 Study #2

As a second method of obtaining an upper bound on the SEM centroid resolution, we again select time periods in which the beam position is observed to be relatively constant, as was the case in the spill range show in Figure 5. As mentioned previously, the RMS variation of measured beam position during such a time interval is the sum of device resolution and beam wandering effects. We select a large number of such time intervals, measuring the RMS variations observed by the SEM and BPM for each time interval. These time intervals' data are summarized in Table 4. If an infinitely large number of time intervals could be selected, it might be expected that the effect of beam wandering would be negligible in some of them, *i.e.*:  $\sigma_{wander} = 0$ , and the observed RMS variation is simply due to the device resolution. Thus, the smallest measured value of  $\sigma_{SEMtot}$  can be used as an upper bound for the SEM resolution:

$$\sigma_{SEM} < 89\mu\text{m} \quad (4)$$

The above argument also holds for deriving an upper bound on the BPM resolution. However, the two upper bounds are not directly comparable because of the scale factor between SEM and BPM referred to previously. After correcting for the scale difference, the SEM always shows the lower spread than the BPM, as shown in the last two columns of Table 4.

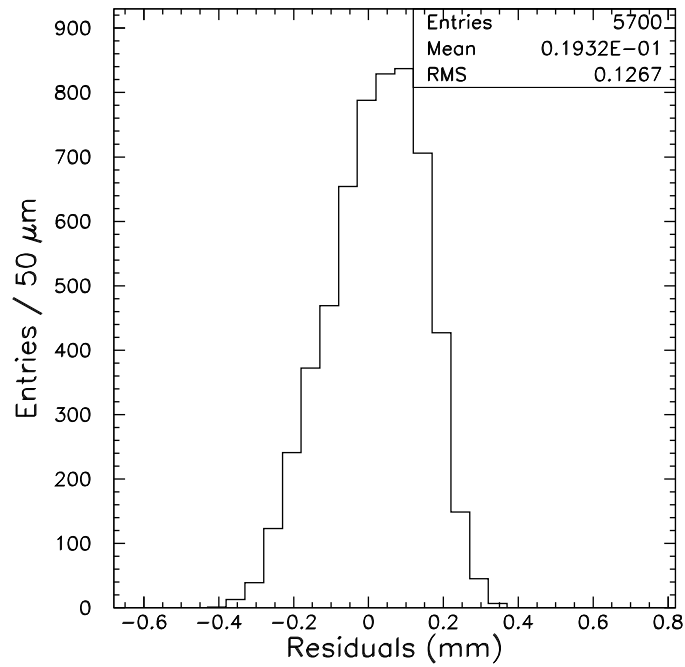
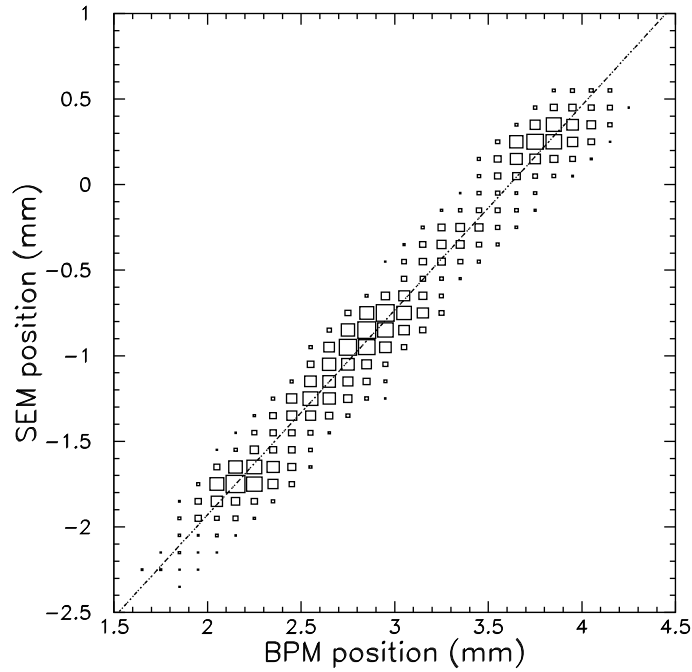


Figure 3: Scatter plot of vertical beam positions measured by the BPM vs that measured by the SEM (top) and the residuals to the best fit line (bottom). From residuals we can infer that the sum in quadrature of BPM and SEM precision is  $127\mu m$ . The spill range for this data is from 7500-13200.

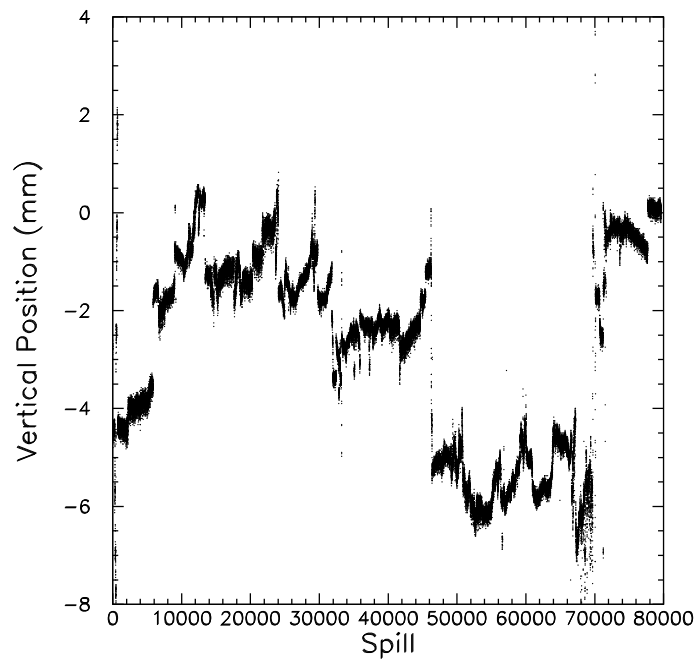
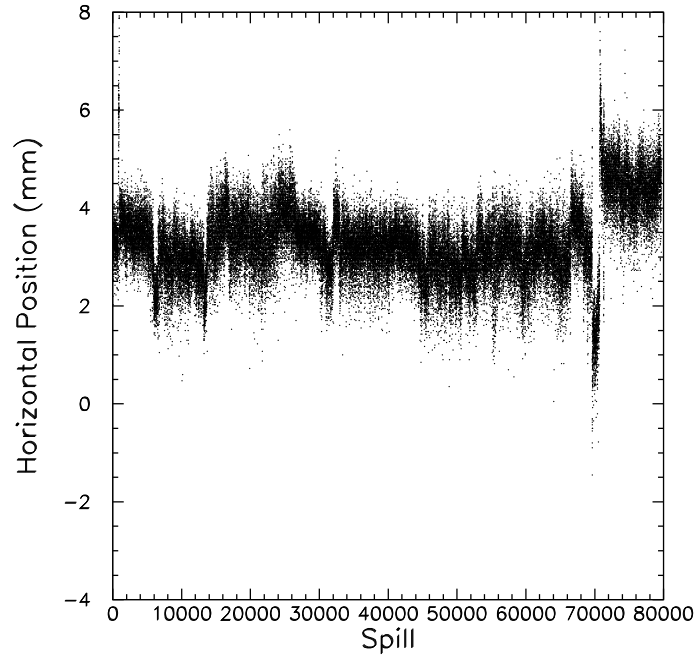


Figure 4: Horizontal (top) and vertical (bottom) beam position plotted versus the spill number.

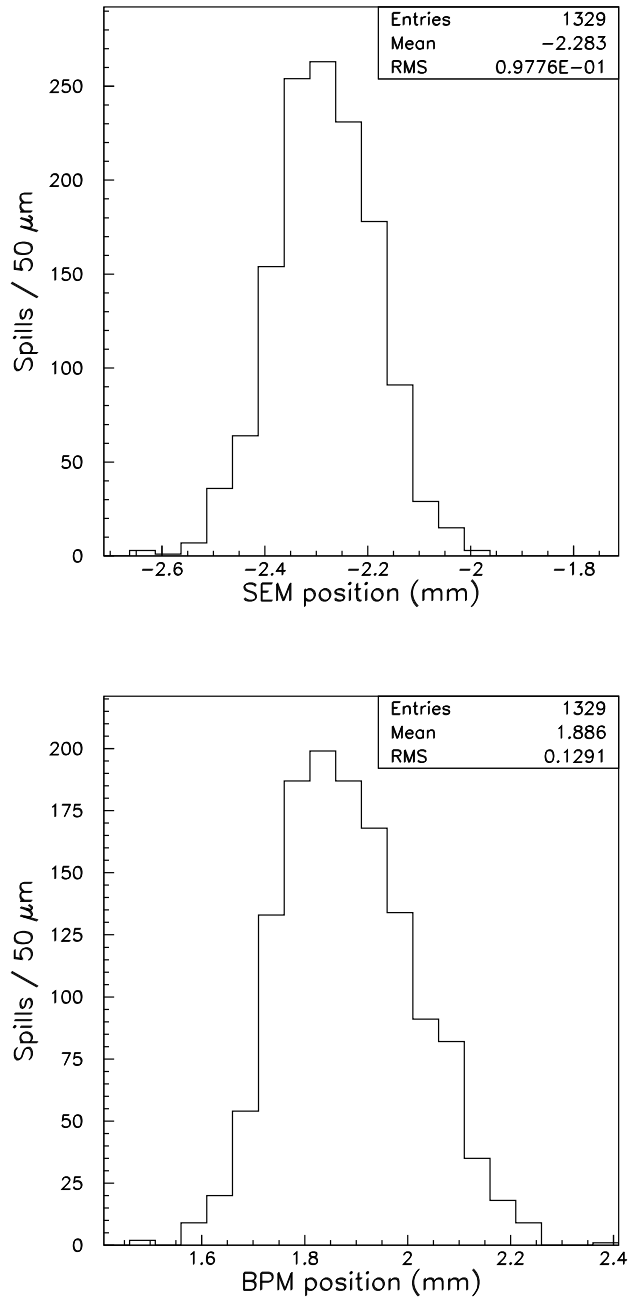


Figure 5: Comparison of the SEM (top) and BPM (bottom) data for the period when beam is continuously hitting almost the same spot (Spill range: 35910-37240). For the same data SEM measurements show smaller spread than BPM. To compare these numbers one needs to know the scale factor between SEM and BPM. For this interval the slope is 1.1 and we need to multiply the BPM residuals with that which makes the difference even bigger. This, however, is not the true resolution of the devices since it also contains some beam wandering.

Spill range	Vertical position on SEM (mm)	$\sigma_{SEMtot}$ ( $\mu m$ )	$\sigma_{BPMtot}$ ( $\mu m$ )	$\sigma_{Total}$ ( $\mu m$ )	$\alpha$	$\sigma_{beam}$ (mm)	$\sigma_{beam}$ spread	Intensity ( $\times 10^{12} ppp$ )	$\sigma_{SEM}$ ( $\mu m$ )	$\sigma_{BPM}$ ( $\mu m$ )
1000-2230	-4.194	125	139	109	0.98	3.30	0.022	4.00	67	88
2230-5120	-3.774	134	142	109	0.98	3.29	0.028	4,00	72	83
6800-8950	-1.862	187	173	126	1.19	3.45	0.045	4.26	65	91
9000-9750	-0.977	166	165	126	1.19	3.46	0.033	4.27	50	97
18800-20287	-1.516	133	143	131	1.19	3.54	0.028	4.60	54	100
20287-21693	-1.026	141	150	131	1.19	3.54	0.029	4.63	51	101
21693-23380	-0.524	156	158	131	1.19	3.54	0.029	4.62	55	100
33500-35050	-2.6	165	162	122	1.1	3.31	0.026	3.89	72	90
35910-37240	-2.316	98	129	122	1.1	3.35	0.023	3.94	47	102
37320-41650	-2.343	135	146	122	1.1	3.39	0.027	3.95	60	96
41750-44650	-2.529	221	211	122	1.1	3.37	0.027	3.90	70	91
48750-50320	-4.758	218	194	127	1.14	3.53	0.030	4.69	86	82
50850-51950	-5.262	187	174	127	1.14	3.54	0.028	4.69	77	89
51950-55000	-5.635	146	150	127	1.14	3.57	0.032	4.66	64	96
60050-60950	-4.751	118	131	127	1.14	3.49	0.026	4.61	62	97
60950-63700	-5.301	129	142	127	1.14	3.50	0.027	4.65	57	99
63900-65000	-4.376	137	149	127	1.14	3.48	0.029	4.65	55	100
72300-75300	-0.49	126	139	138	1.08	3.50	0.031	4.54	79	105
77700-79659	-0.122	89	126	138	1.08	3.46	0.032	4.67	64	113

Table 4: Vertical SEM and BPM spreads for intervals during which beam wandering is small along with the residuals and the slope from SEM vs BPM scatter plots of data encompassing those intervals.

Note that the upper bound on the SEM resolution obtained in this study, 89  $\mu m$ , is consistent with the 90  $\mu m$  upper bound found in “Study #1”.

### 3.3 Study #3

The last estimate of the SEM resolution attempts to combine the data from the previous two estimates to get the true resolution. This means we must properly estimate the scale factor difference in the first study and also the beam wandering effect from the second study. The second study gave, during short time intervals, measures of:

$$\sigma_{SEMtot}^2 = \sigma_{wander}^2 + \sigma_{SEM}^2 \quad (5)$$

$$\sigma_{BPMtot}^2 = \sigma_{wander}^2 + \alpha^2 \cdot \sigma_{BPM}^2$$

where we have added the factor  $\alpha^2$  in front of the  $\sigma_{BPM}$  to accommodate for the scale factor between SEM and BPM. The slope  $\alpha$  is not universal and is different for different sets of data. This fact suggests that its origin is not a simple electronics scale factor, but is instead perhaps a non-linearity in the BPM or the result of imperfections in the foil SEM strip pitches at different locations on the foil or some other irregularities.

First we look for the interval during which the beam moved around and within that data we look at the periods when beam wandering was small. From the SEM versus BPM data in Figure 3 we can find the best fit line and the residuals  $\sigma_{res} = 127 \mu m$ . Both  $\sigma_{BPM}$  and  $\sigma_{SEM}$  contribute to residuals. We can write:

$$\sigma_{res}^2 = \alpha^2 \cdot \sigma_{BPM}^2 + \sigma_{SEM}^2 = (127 \mu m)^2 \quad (6)$$

where  $\alpha \sim 1.1$  is the slope between SEM and BPM ( $SEM = \alpha \cdot BPM + const.$ ) observed in Figure 3.

Second, as we have seen before from looking at the data for SEM and BPM separately during periods in which the beam does not move appreciably, we can find  $\sigma_{SEMtot}$  and  $\sigma_{BPMtot}$ , which includes a contribution from beam wandering. Using the data from Figure 5,

$$\sigma_{SEMtot}^2 = \sigma_{wander}^2 + \sigma_{SEM}^2 = (97 \mu m)^2 \quad (7)$$

$$\sigma_{BPMtot}^2 = \sigma_{wander}^2 + \alpha^2 \cdot \sigma_{BPM}^2 = (129 \mu m)^2$$

or combining the above two expressions in Equation 7 we have

$$\alpha^2 \cdot \sigma_{BPM}^2 - \sigma_{SEM}^2 = (129 \mu m)^2 - (97 \mu m)^2 \quad (8)$$

Combining Equations 6 and 8 we may solve for the SEM centroid resolution, and assuming  $\alpha = 1.1$  we may obtain the BPM resolution as well:

$$\begin{aligned} \sigma_{SEM} &= 67 \mu m \\ \sigma_{BPM} &= 98 \mu m \end{aligned}$$

We have repeated this sort of analysis of the vertical beam data for several time intervals and the results are shown in Table 4. The observed resolutions are not constant, with the variation due possibly beam-related effects or variation in resolution across the aperture of the SEM or BPM. The average values for the resolutions that we get are:  $\sigma_{SEM} = 64 \mu m$  and  $\sigma_{BPM} = 96 \mu m$ .

In the horizontal plane the beam was wandering much larger than in the vertical plane. Because of this setting up the upper limit for the resolution as we did for the vertical plane wasn't that useful. The beam width also was not as constant as in vertical plane. It varied around two different beam widths, 7.4 mm and 8.2 mm, correlated with two different beam intensities. The SEM error for those two beam widths is quite different, so we split data in two sets. We looked at 32 intervals with 1000 spills each. We assumed that the BPM resolution for the horizontal plane is the same as for the vertical. In each interval we could find beam wandering ( $\sigma_{wander}$ ) from the BPM measurements and then plug that into SEM data and find  $\sigma_{SEM}$ . As a result we find:

$$\sigma_{SEM}(\sigma_x = 7.4mm) = 151 \mu m \quad (9)$$

$$\sigma_{SEM}(\sigma_x = 8.2mm) = 171 \mu m \quad (10)$$

These results have bigger error than the result for the vertical plane since here we had to assume what is the resolution of the BPM. Correlating data with BPM was also harder for the horizontal plane since there were magnets in between the SEM and the horizontal BPM. Table 5 summarizes horizontal data.

Spill range	Horizontal position on SEM (mm)	$\sigma_{SEMtot}$ ( $\mu m$ )	$\sigma_{BPMtot}$ ( $\mu m$ )	$\sigma_{res}$ ( $\mu m$ )	$\alpha$	$\sigma_{beam}$ (mm)	$\sigma_{beam}$ s pread	Intensity ( $\times 10^{12}$ )	$\sigma_{SEM}$ ( $\mu m$ )
1000-2000	3.67	373	516	164	0.65	7.40	0.34	4.00	175
2000-3000	3.56	371	505	137	0.68	7.43	0.35	4.01	155
3000-4000	3.45	375	475	122	0.74	7.40	0.40	3.99	145
4000-5000	3.52	371	484	126	0.72	7.47	0.37	4.01	145
7000-8000	3.03	522	711	157	0.70	7.52	0.47	4.27	169
8000-9000	2.89	493	632	136	0.75	7.50	0.51	4.24	150
9000-10000	2.97	468	599	150	0.74	7.51	0.50	4.26	163
10000-11000	2.89	416	543	129	0.74	7.45	0.49	4.18	124
11000-12000	2.97	393	508	128	0.73	7.43	0.42	4.14	145
12000-13000	2.79	415	540	134	0.73	7.36	0.40	4.13	150
26700-27700	3.45	332	423	118	0.74	7.42	0.38	4.14	136
27700-28700	3.45	354	454	122	0.74	7.43	0.39	4.13	134
28700-29700	3.47	323	416	127	0.72	7.37	0.33	4.07	143
29700-30700	3.2	424	557	126	0.73	7.40	0.35	4.11	142
40000-41000	3.22	391	498	157	0.72	7.20	0.31	3.94	172
41000-42000	3.31	379	489	145	0.72	7.17	0.30	3.93	161
42000-43000	3.26	367	487	135	0.70	7.12	0.28	3.91	152
43000-44000	3.13	369	486	139	0.70	7.13	0.30	3.90	156
50800-51800	2.92	446	612	164	0.68	8.16	0.55	4.69	175
51800-52800	2.69	442	598	150	0.70	8.24	0.62	4.67	160
52800-53800	3.19	502	654	169	0.73	8.11	0.61	4.63	179
53800-54800	3.06	402	531	173	0.69	8.26	0.61	4.68	179
56000-57000	3.19	477	587	155	0.77	8.13	0.67	4.60	165
57000-58000	3.25	476	585	150	0.77	8.14	0.78	4.59	178
58000-59000	3.11	464	585	153	0.75	8.08	0.70	4.58	166
61000-62000	3.08	440	557	167	0.73	8.14	0.56	4.66	182
62000-63000	3.26	449	586	146	0.72	8.16	0.66	4.66	162
63000-64000	3.16	455	580	144	0.75	8.12	0.70	4.64	158
74600-75600	4.34	498	618	144	0.77	7.95	0.55	4.55	161
75600-76600	4.27	492	641	152	0.73	8.12	0.61	4.61	162
76600-77600	4.42	478	585	167	0.76	8.19	0.73	4.67	186
77600-78600	4.31	448	579	165	0.74	8.25	0.79	4.67	157
78600-79600	4.50	497	624	149	0.74	8.17	0.65	4.67	192

Table 5: Horizontal SEM and BPM spreads for intervals during which beam wandering is small along with the residuals and the slope from SEM vs BPM scatter plots for those intervals. The SEM precision is calculated using the assumption that horizontal BPM precision is the same as in vertical BPM ( $\sigma_{BPM} = 96\mu m$ ).

## 4 Expected SEM Resolution

The previous section measured the centroid resolution at three different beam widths. A less reliable estimate was also made of the beam width resolution. These device resolutions are affected by several instrumental factors[4]:

- The error in foil strip positions
- The absolute and relative errors on the signal amplitude measurement (signal noise).
- The number of strips per beam  $\sigma$
- The data analysis method, e.g. what kind of a fitting function is used...

The last three effects listed above smear the pulse height  $y_i$  observed on an individual strip  $i$  by an amount  $\delta y_i$ . The first effect, which arises due to the fact that the foil strips are not perfectly positioned on the grid, causes a smearing of the actual position  $x_i$  of the strips. This form of strip placement error we accounted for using the following: we assumed an additional uncertainty on the strip pulse heights of  $\delta y_i = f'(x) \cdot \delta x_i$  where  $f'(x)$  is the derivative of the fitting function that we use to describe the beam profile and  $\delta x_i$  is the uncertainty in the strip positions.

Signal noise from the SWIC electronics smears the pulse height  $y_i$  for each foil strip, and this readout error is another cause of the SEM centroid error. The noise can be split in two components, one that does not depend on the signal and the other that does. The former we call absolute error and latter relative error. Figure 6 shows gaussian beam profile curves with error bands overlaid with our real data from this beam test. For the error bands, absolute and relative uncertainties on the strip pulse heights are chosen, as we will see later, to roughly fit the resolutions that were found in previous section. Inspection of these graphs reveals that the SWIC readout electronics probably have some combination of absolute and relative electronics noise, since the scatter appears both in the peak and in the tails of the beam profiles.

### 4.1 Beam Centroid Resolution

We use the data from the MiniBooNE test to estimate the electronics noise present. In Figure 7 is shown the expected SEM centroid resolution (in millimeters) as a function of the absolute and of the relative pulse height uncertainty. This curve is derived from a calculation. The calculation is accomplished using a series of 1000 gaussian distributions loaded into HBOOK histograms in PAW, with the histograms containing 44 bins to simulate the 44 strips of our SEM's which sample the beam intensity. Each bin of the 1000 histograms are filled with a Gaussian-weighted pulse height  $y_i$  which is then smeared randomly by an amount  $(\delta y_i)^2 = (\epsilon \cdot y_i)^2 + \delta^2$ , where  $\epsilon$  represents the relative uncertainty and  $\delta$  represents the absolute uncertainty. The 1000 histograms are fitted with Gaussian curves. The centroid resolution reported in Figure 7 is the sum in quadrature of the uncertainty from the fit and

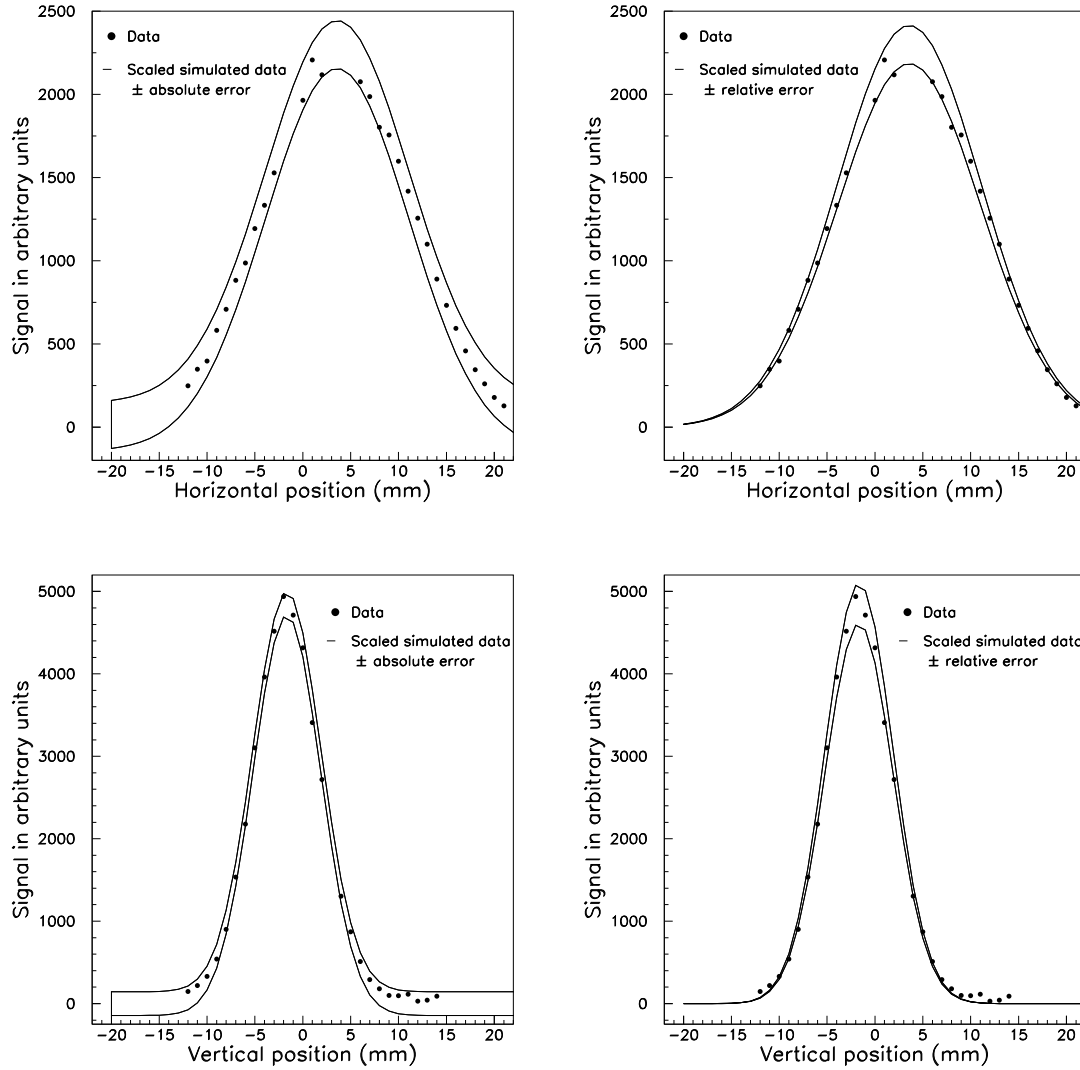


Figure 6: Simulated Gaussians with  $\sigma = 7.5mm$  (top) and  $\sigma = 3.55mm$  (bottom) and with absolute (left) and relative error (right). The simulated data is scaled to the area of the real data that is overlaid. The absolute error in these plots is 144 in arbitrary units and relative error is 4%. The real beam data is the same as that in Figure 2.

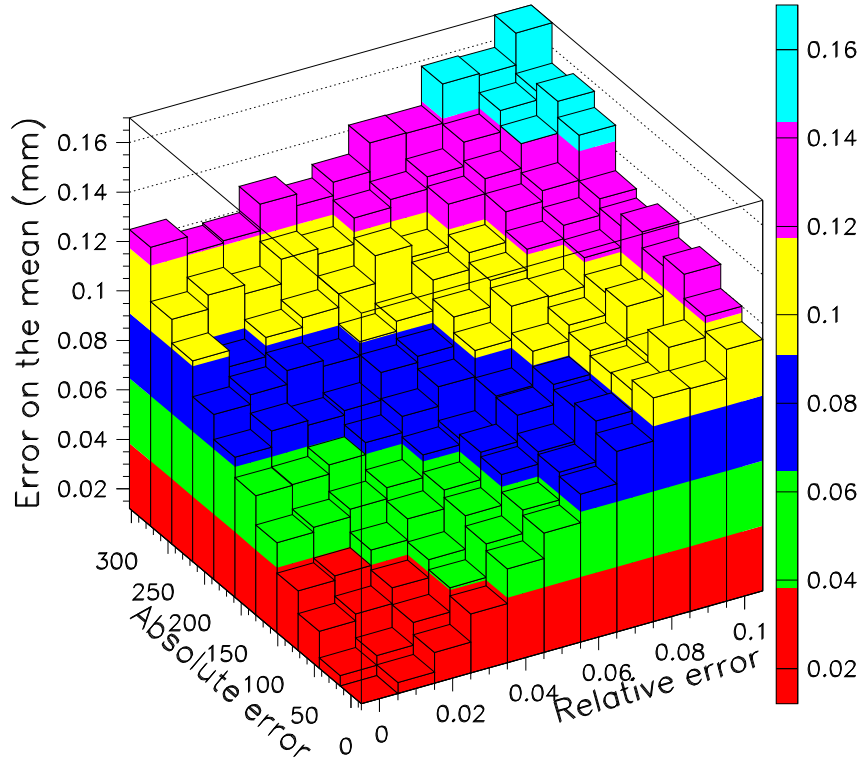


Figure 7: Error on the mean from simulated data as a function of the absolute and relative error when the beam width is  $\sigma_{beam} = 3.5$  mm, which is approximately what the beam width in vertical plane was during the MiniBooNE prototype study. The contour shown is derived from a calculation described in the text.

the difference between the true and fitted centroid positions. The 1000 histograms used to make the contour in Figure 7 all had an assumed beam width of 3.5 mm, but with varying absolute or relative pulse height uncertainties. Our beam test data from the 3.5 mm wide beam indicated a resolution of  $\sim 65 \mu\text{m}$ . From this value, we may infer a family of possible absolute and relative pulse height uncertainties for the SWIC electronics ranging from an absolute pulse height uncertainty of  $\delta = 300$  and relative uncertainty of  $\epsilon = 0\%$  to an absolute pulse height uncertainty  $\delta = 0$  and relative uncertainty of  $\epsilon = 10\%$ .

Using the other measured resolutions at other beam widths allows us to determine the appropriate absolute and relative pulse height uncertainties from the electronics. In Figure 8 we show the calculation of expected SEM centroid resolution as a function of beam width  $\sigma_{beam}$  for two extreme choices of pulse height uncertainty:  $\delta = 300$  and  $\epsilon = 0.00$  as well as  $\delta = 0$  and  $\epsilon = 0.10$ . In this figure, the area of the simulated beam profiles is held constant

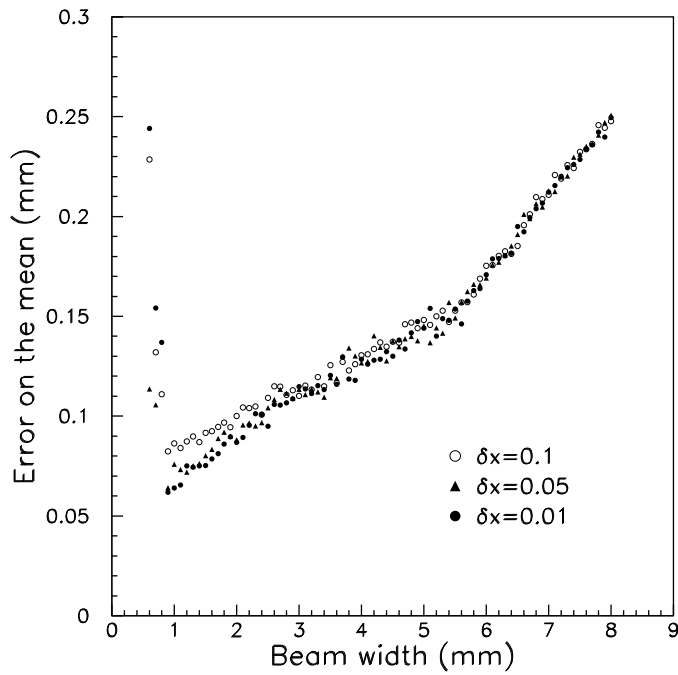
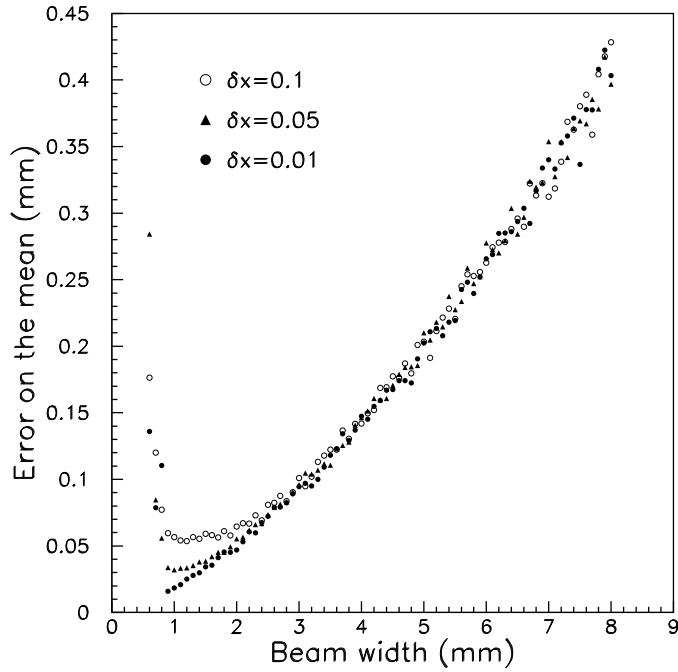


Figure 8: Error on the mean calculated from simulated data for different beam widths. Beam distributions were generated with some noise. Top plot shows the case when absolute error is 300 in arbitrary units and relative error is 0 and bottom plot shows the case when absolute error is 0 and relative error is 10%.  $\delta x$  is the amount by which strip position was randomly varied in the calculation.

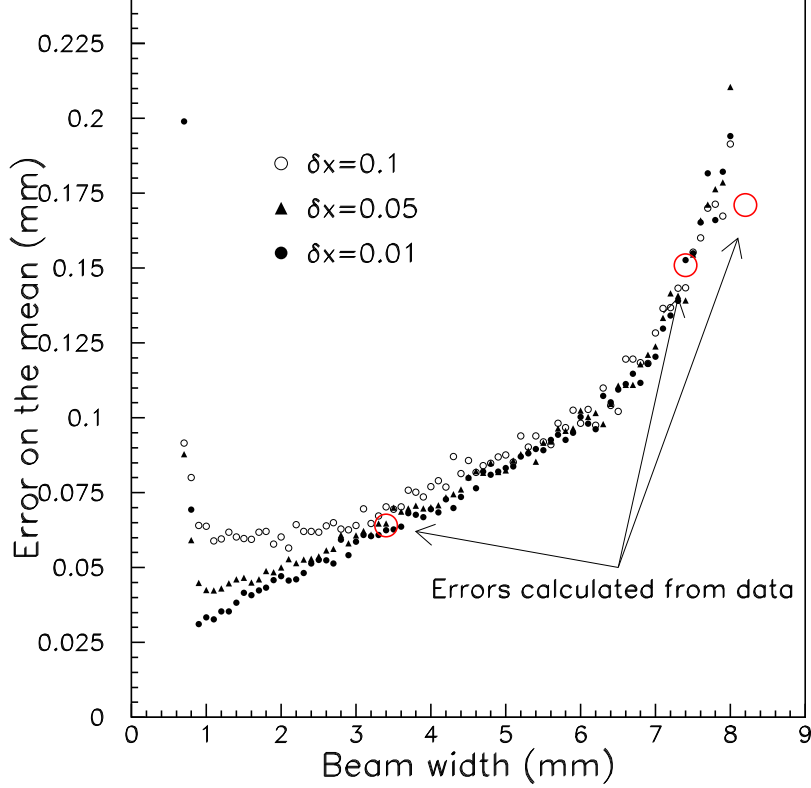


Figure 9: Error on the mean calculated from the simulated data for different beam widths.  $\delta x$  is the amount by which strip position. It's effect is important for smaller beam widths. The absolute error  $\delta = 58$  in this plot and the relative error is  $\epsilon = 4\%$ . The errors were chosen so that they approximately fit the resolutions that were found in section 3.

(area is proportional to beam intensity), so that smaller beam widths result in larger pulse height strips as compared to broader beam widths. As can be seen, a smaller centroid resolution is anticipated for narrower beams, until the beam width  $\sigma_{beam} = 1.0$  mm, which corresponds to the strip-to-strip spacing for our SEM. As the beam becomes narrower, the centroid resolution is more sensitive to the placement accuracy  $\delta x_i$  of the strips in the SEM grid. Our calculation is performed for three different accuracies,  $\delta x_i = 10, 50,$  and  $100 \mu\text{m}$ . We expect  $\delta x_i = 50 \mu\text{m}$  for the prototype and  $\delta x_i = 10 \mu\text{m}$  will be achieved for the final NuMI SEM's. Our test beam data are superimposed on our calculated resolution in Figure 9, where the best fit values of  $\delta = 58$  and  $\epsilon = 0.05$  have been derived from the three data points shown at  $\sigma_{beam} = 3.5, 7.4,$  and  $8.2$  mm. This figure indicates a resolution of order  $20\text{-}30 \mu\text{m}$  may be anticipated in the NuMI beam line, where the beam width  $\sigma_{beam} \sim 1.0$  mm.

Figure 10 shows a calculation which estimates how the variation of the beam intensity

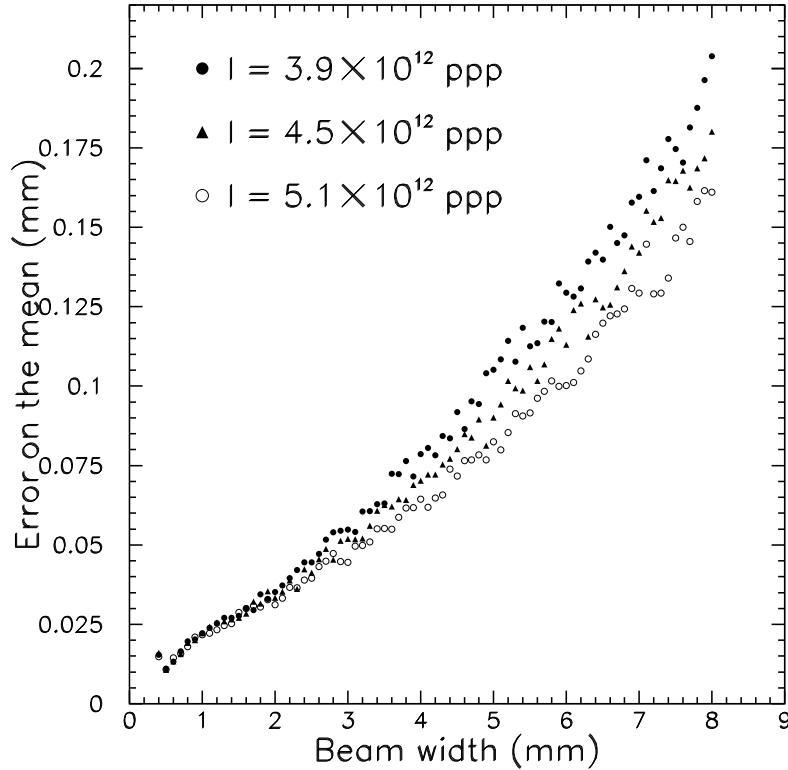


Figure 10: Error on the mean simulated for different beam intensities. Absolute error in this plot is 58 in arbitrary units and the relative error is 4%.

during the course of the MiniBooNE test affects the derived SEM centroid resolutions. The data taken at  $\sigma_{beam} = 3.5$  had spill intensities of order  $4.0 - 4.6 \times 10^{12}$  ppp, the data at  $\sigma_{beam} = 7.4$  was at  $4.0 \times 10^{12}$  ppp, while the data at  $\sigma_{beam} = 8.2$  was at  $4.6 \times 10^{12}$  ppp. Thus, the fact that our data point in Figure 9 at  $\sigma_{beam} = 8.2$  mm is a little lower than the calculated curve is consistent: while the spread in intensities does not contribute strongly to the beam position resolution at  $\sigma_{beam} \sim 3$  mm, it does affect the resolution at the 10% level at  $\sigma_{beam} \sim 7 - 8$  mm.

Figure 11 show how does error on the mean depend on the absolute and relative errors. Those two graphs are for two different beams with same intensity but different width. Narrower beam has larger signals on fewer strips so the absolute error does not affect it like it does a wider beam.

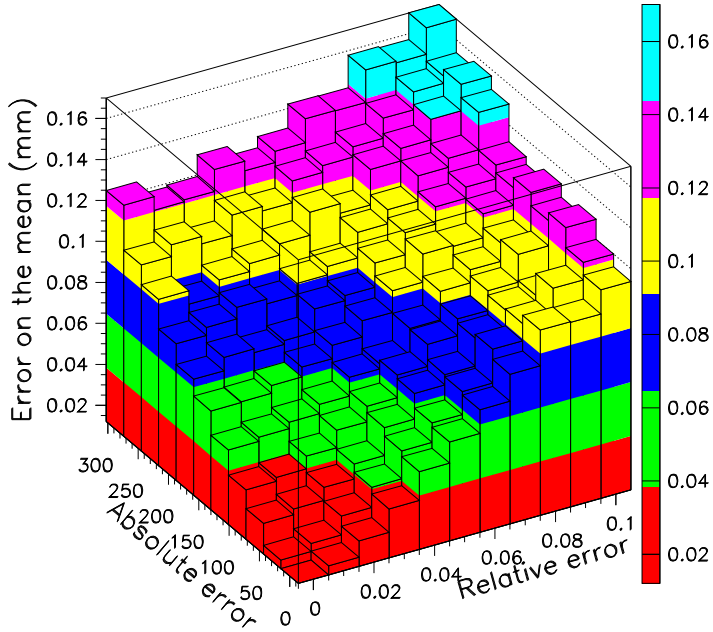
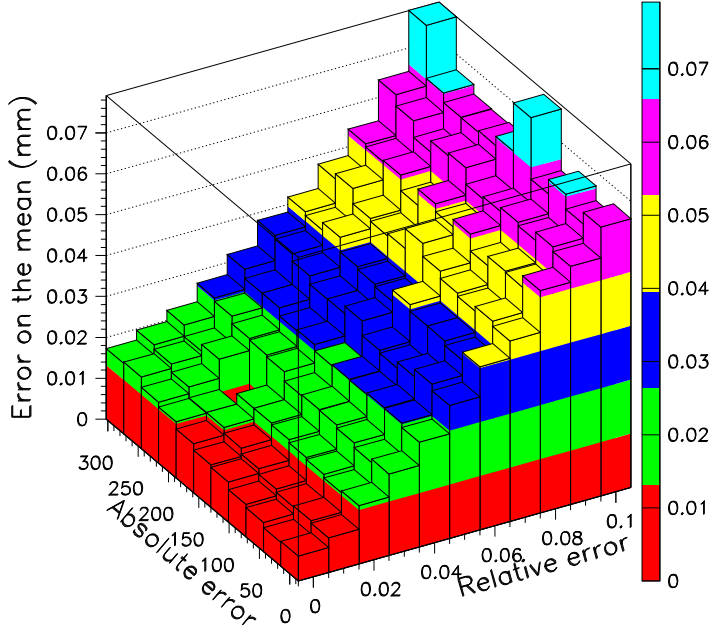


Figure 11: Error on the mean from simulated data as a function of the absolute and relative error. For the top plot the beam width is  $\sigma_{beam} = 1$  mm like it will be in NuMI and for the bottom plot  $\sigma_{beam} = 3.5$  mm which is approximately what the beam width in vertical plane was during the prototype study. The generated Gaussian beam profiles used to make both contours had the same area (beam intensity).

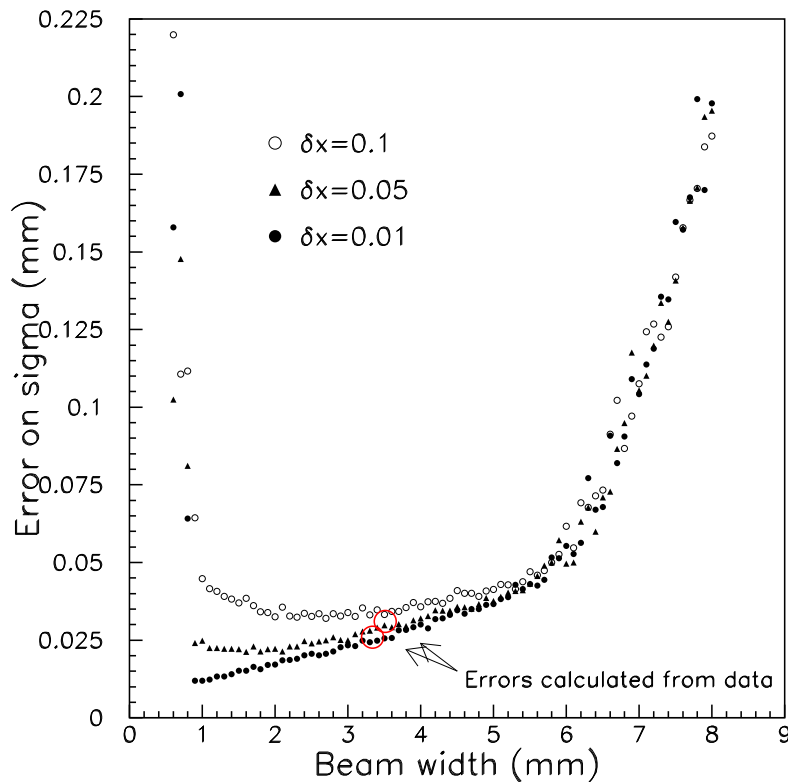


Figure 12: Error on the beam width from simulated data as a function of the beam width. Constant Intensity is assumed. The calculations assume strip readout pulse height uncertainties of  $\delta = 29$  and  $\epsilon = 0.02$ . Overlaid on the calculated curves are two points derived from the MiniBooNE test data measured at beam width of about 3 mm.

## 4.2 Beam Width Resolution

We have also used the above estimation procedure to understand the expected resolution on the beam width measured by the SEM grid. Figure 12 shows the expected resolution on the beam width as a function of the beam width. As with the mean, the uncertainty on the beam width diverges sharply as the beam width falls below the strip pitch of 1.0 mm.

Overlaid on the plot in Figure 12 are two points derived from the MiniBooNE test beam run which are the variation of the width in the vertical plane as observed over two beam spill ranges. This is analogous

In order to best accommodate the experimental points, the beam width resolution is calculated using the absolute pulse height error  $\delta = 29$  and relative pulse height error  $\epsilon = 0.02$ .

We note that these pulse height errors are somewhat different than the values derived from the centroid resolution study. In Figure 13, we fit both the centroid resolution and

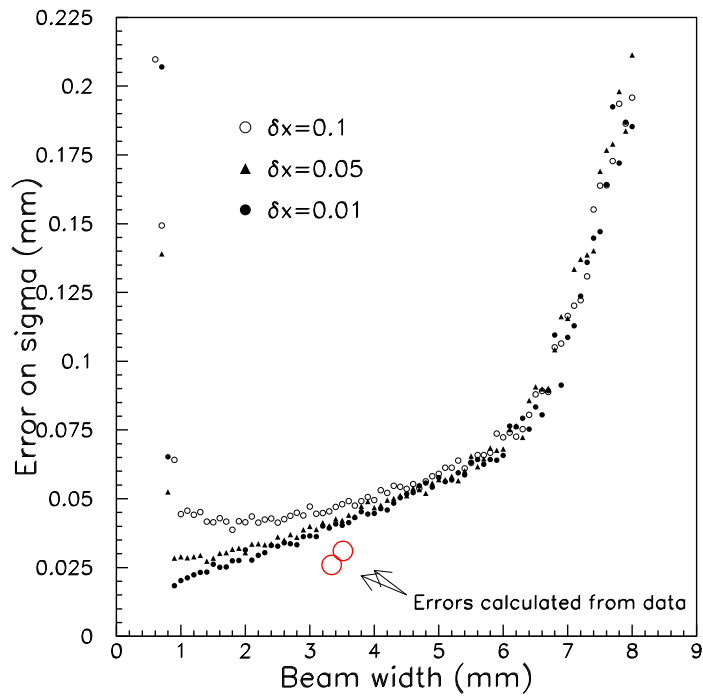
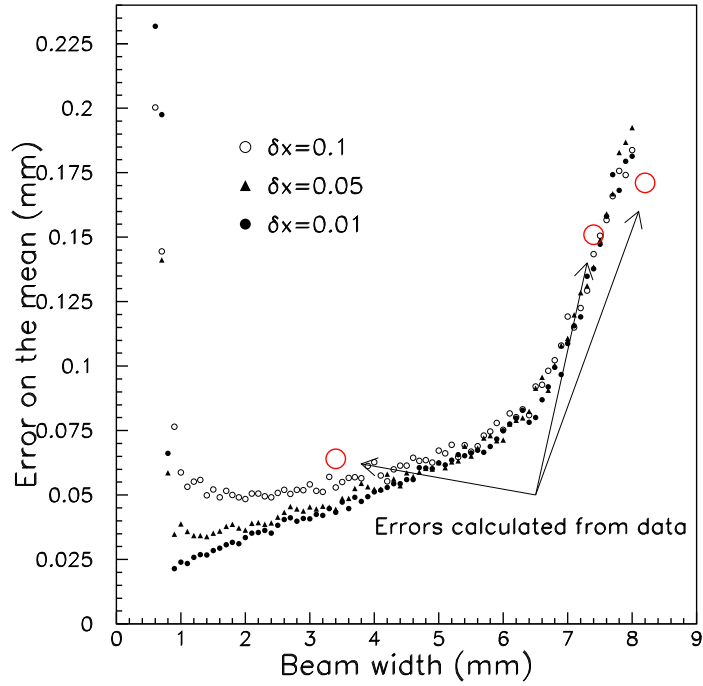


Figure 13: Error on the beam centroid (top) and width (bottom) from simulated data as a function of the beam width. Constant Intensity is assumed. The calculations assume  $\delta = 43$  and  $\epsilon = 0.035$

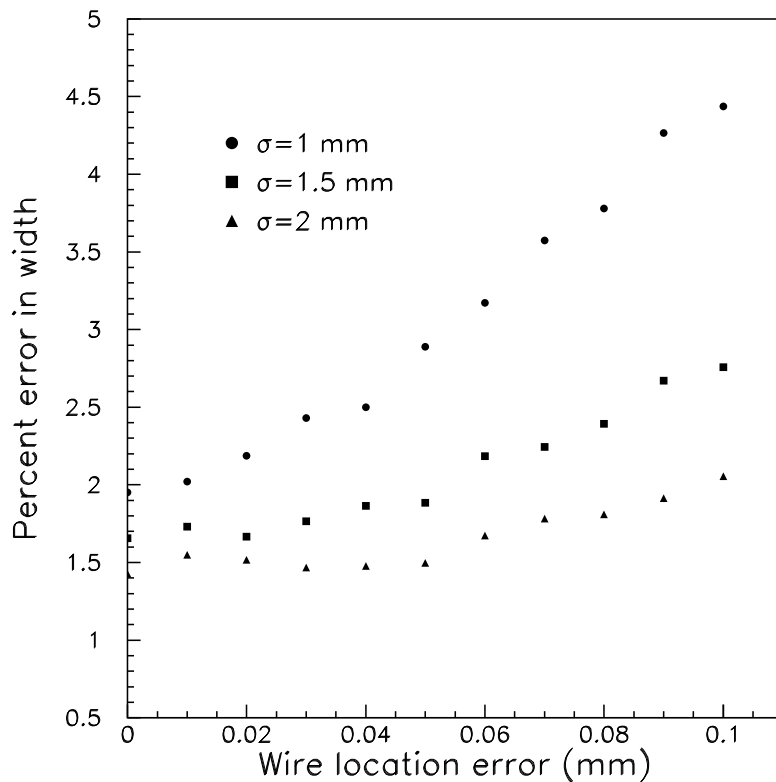


Figure 14: Error on the beam width from simulated data as a function of the foil strip placement accuracy, for beam widths of 1.0, 1.5, and 2.0mm. Constant Intensity is assumed. The calculations assume strip pulse height uncertainties  $\delta = 43$  and  $\epsilon = 0.035$ .

the width resolution data to find the best values of the pulse height uncertainties. The best values that describe these two data sets are  $\delta = 43$  and  $\epsilon = 0.035$ . It appears that these pulse height errors can bisect the resolutions of the mean and width measured in the MiniBooNE test, but these pulse height error values do not entirely satisfactorily describe the two data sets.

Figure 14 shows how the width resolution varies as a function of the accuracy of placing the foil strips on the grid frame. This is shown for  $\delta = 43$  and  $\epsilon = 0.035$ , the 'best fit' value for the pulse height uncertainties derived from our beam width and beam centroid resolutions measured from the MiniBooNE data. The curve is generated for three beam widths, 1.0, 1.5, and 2.0 mm. Only since it has a stronger effect in the signal peak.

Figure 15 shows how the width resolution varies as a function of the relative and absolute pulse height uncertainty in the electronics readout. The contour plots shown are for a 1 mm and 3 mm beam size, representative of the NuMI and MiniBooNE beams, respectively. The

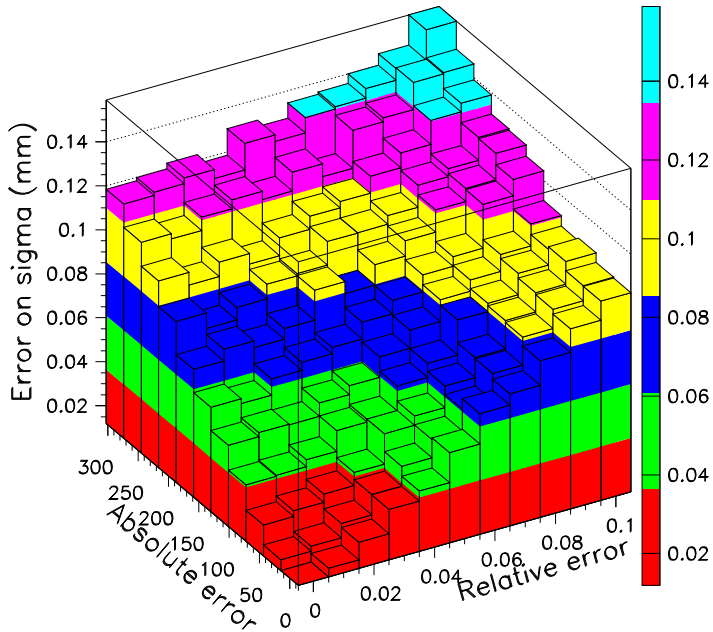
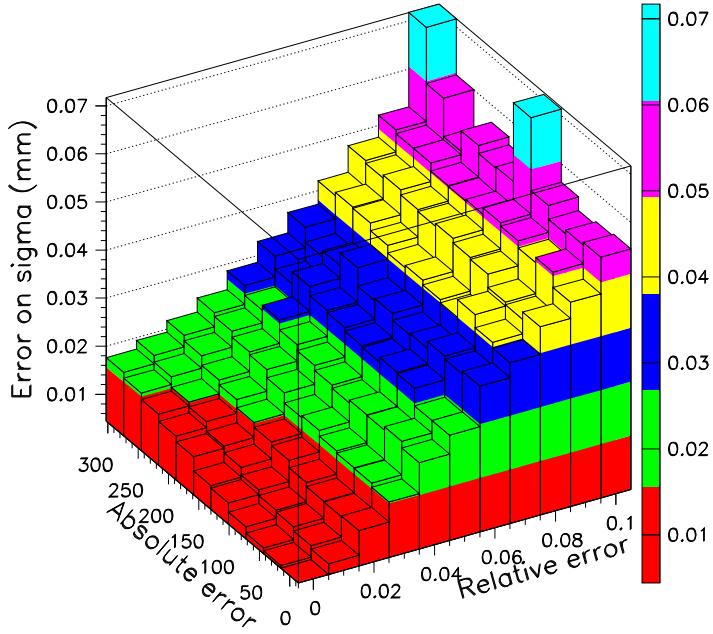


Figure 15: Error on the beam width from simulated data as a function of the absolute and relative pulse height error. For the top plot the beam width is  $\sigma_{beam} = 1$  mm like it will be in NuMI and for the bottom plot  $\sigma_{beam} = 3.5$  mm which is approximately what the beam width in vertical plane was during the prototype study. The generated Gaussian beam profiles use to make both contours had the same area (beam intensity).

contour shapes are quite similar to those for the beam centroid resolutions, namely that at large beam sizes both the absolute and the relative uncertainty contribute strongly to the beam width resolution, while for the smaller beam size the relative uncertainty contributes most str

What should be clear from the results of this section is that the beam centroid or width resolution depends critically on the electronics readout of the SEM. The electronics smearing of the strip pulse heights is, for most beam configurations, a more important factor than the mechanical features of the SEM grid itself. Only for beam sizes which are small or comparable to the SEM grid spacing does the mechanical assembly contribute substantially to the resolution.

## 5 Conclusion

From the prototype data we observe that the beam centroid resolution of the 1 mm pitch SEM prototype is around  $64\mu\text{m}$  for the beam with  $\sigma = 3.5\text{mm}$ . From the extrapolation in Figure 9 to beam widths relevant for NuMI, we anticipate a centroid resolution of 20-30  $\mu\text{m}$  for a 1 mm beam. Although the beam intensity will be a factor of 5 larger in the NuMI beam, which might be expected to improve the SEM resolution due to increased signal size, this signal increase will be compensated by a signal decrease arising the narrower foil strip size in the NuMI SEM's. Thus, the extrapolation shown in Figure 9 should be approximately correct.

The two SEM's just upstream of the NuMI target will have finer pitch than the prototype SEM (0.5 mm compared to 1.0 mm), and also wider strips (0.25mm as compared to the 0.15mm of the transport line SEM's). One therefore expects that (a) the mechanical assembly details of the 0.5mm SEM's shall not be as critical, since the beam size will be larger than the strip spacing, and (b) the pulse height smearing will not as greatly affect their resolutions because the wider strips will yield a 1.7 times greater signal. The results of the present study suggest that these 0.5 mm SEM's should behave in a 1.0 mm beam much like the 1.0 mm prototype performance for a 2.0 mm beam. That is, an approximate scaling relation should exist with strip pitch.

## 6 Acknowledgements

The beam test described in this memo was performed thanks to the efforts of many people. Much mechanical and vacuum re-working of the device was done by Cary Kendziora of the FNAL Particle Physics Division. Sam Childress, Rick Ford, Gordon Koizumi from the NuMI Department, and Gianni Tassotto from the Accelerator Division Instrumentation Department installed the SEM and ran the test. Tom Kobilarcik and Craig Moore from MiniBooNE and the Extracted Beams Department assisted with integration into the 8 GeV line and also getting access to the data from the MiniBooNE data stream.

## References

- [1] Sacha E. Kopp, Marek Proga “Design of the Prototype NuMI Profile Monitor SEM”, NuMI-B-933 (2003)
- [2] D. Indurthy *et al*, “Profile Monitor SEM’s for the NuMI Beam at FNAL”, *Proceedings of the 11<sup>th</sup> International Beam Instrumentation Workshop (BIW04)*, AIP Conference Proc. **732**, pg 341-349 (2004).
- [3] The SEM pulse height is nominally a charge whose magnitude should be of order a percent times the number of primary beam particles traversing a foil strip. These pulse heights, amounting to picoCoulombs of charge in our test, were read out using charge-integrating amplifiers whose gain and charge-to-voltage conversion were not well known for our test. The vertical scales are actually millivolts as read out by the charge-integrating electronics, but the exact gain of the electronics. We list all pulse heights in arbitrary units, since the fundamental units are not well known and these are not important for our final results.
- [4] Mike Plum “Interceptive Beam Diagnostics-Signal Creation and Materials Interactions”, *Proceedings of the 11<sup>th</sup> International Beam Instrumentation Workshop (BIW04)*, AIP Conf. Proc. **732**, Knoxville, TN (2004).